FOLDED SIDEBAND-RESONANT OUTPUT MODE CLEANER FOR LIGO 2K IFO

GREGORY F SNYDER AND RICHARD GUSTAFSON

ABSTRACT. I investigate a folded sideband resonant output mode cleaner for the LIGO two-kilometer interferometer. Four successive optical table-based triangular 10-meter OMC cavities have been built which resonate sidebands at 29 MHz; we started with a 2.5 meter one-fold cavity, and presently have a 45-inch five-fold cavity. A carrier-based dither lock was implemented and the cavity behavior studied; locks are minutes in duration. A sideband-based, carrier independent dither lock was devised. Alignment and noise have been challenging; we estimate a length noise of order 1 nanometer. The noise-induced conversion fraction of a phase modulated carrier-sideband test signal (token noise process) is reported and analyzed.

1. INTRODUCTION

A mode cleaner is a Fabry-Perot optical cavity which filters light in both frequency and spatial propagation mode (cite Siegman). The Laser Gravitational Wave Observatory (LIGO) project uses mode cleaners to enhance laser signal qualities, ultimately reducing strain noise. Pre-Mode Cleaners (PMCs) prepare light before it enters the interferometer (IFO) arms. In principle, an Output Mode Cleaner (OMC) can be used to filter light emitted from the IFO. However, OMCs are not in use because previous attempts to use them resulted in additional noise (2).

In this paper I present initial work on a new prototype OMC, carried out at the LIGO Hanford Observatory. The salient features of this OMC are: a) It is designed to resonate the LIGO radio frequency (RF) sidebands *equally* with the carrier, and b) A delay-line was built into the cavity in order to reduce the physical footprint.

The LIGO 2-km interferometer at Hanford (H2) operates using a laser carrier signal with wavelength $\lambda_0 = 1.06\mu m$ and RF sidebands offset from the carrier by frequency $f_{SB} = 29.506876\ MHz$. The beam is split into two Fabry-Perot resonant arms. As the carrier light enters these IFO arms, the sidebands are reflected back into the "power recycling cavity." The carrier light resonates in each of the arms, and recombines at the beamsplitter. While the IFO is locked, a Pound-Drever-Hall (PDH) (3) feedback loop ensures that the recombined beams interfere destructively. In other words, the output beam is centered in a dark interference fringe. Hence the output port of the IFO is called the anti-symmetric (AS) or "dark" port. Perturbations to the length of the IFO arms phase shift the carrier light, moving the interference pattern and causing carrier light to appear at the AS port.

Date: 20 September 2007.

This shift is measured by the beats of the carrier with the RF sidebands. Once this shift is detected, the PDH servo loop corrects it by readjusting the length of the IFO arms. This type of instrument is known as a "null" instrument, because measurements are made by keeping track of changes needed to ensure a null signal.

In practice, noise processes limit the extent to which the AS port can be kept dark. Some noise introduces unimportant frequencies and spatial structure to the emitted light. These features can be confused for arm length perturbations by the PDH servo. This produces unwanted noise in the gravitational strain measurements made by the IFO. A mode cleaner could be used to reject the unimportant noise features.

Previous OMC candidates were not designed to perfectly resonate the RF sidebands. A short prototype OMC resulted in excess noise (2). Some processes of concern include upconversion to sidebands and disruption to relative carrier-sideband phase information. It is thought that an OMC which resonates equally the carrier and sidebands might avoid such processes.

However, a sideband-resonant OMC for the H2 IFO requires a five-meter cavity. It is possible to "fold" such a cavity so that it readily fits on a LIGO optical table. We explore such a design using standard optical elements.

In Section 2 I introduce the physical concepts behind mode cleaners. In Section 3 I describe the physical structure of our OMC cavity design. Section 4 describes two locking techniques, the standard "dither" lock and a carrier-independent "RF dither" lock. Observations are presented and discussed in Section 5. The work is summarized in Section 6. In Appendix A I outline in detail some alignment strategies and observations.

2. Background

This section contains the basic optics of Fabry-Perot mode cleaners and LIGO. For readers well-acquainted with these topics, or for readers seeking discussion of a specific topic, refer to Table 1 at the end of Section 2.4. Much of this background can also be found in *Lasers* by Siegman (1).

2.1. **Gaussian Beam Propagation.**

A laser beam propagating in free space can be regarded a linear combination of Hermite-Gaussian (or Laguerre-Gaussian) spatial mode patterns. (In other words, these patterns form a complete basis for the space of possible laser beam propagation patterns). See Figure 1. The simplest eigenmode is the tranverse electric and magnetic (TEM) 00 mode. This is the optimal mode for the LIGO interferometers, and the mode which carries the cleanest strain information.

For the following, consider a pure TEM 00 beam propagating along the x-axis with wavelength λ. It is a beam with a purely Gaussian transverse intensity profile. Specifically, for a fixed x, where r is the distance from the x-axis:

$$I(r) = I_0(x)e^{\left(\frac{-2r^2}{\omega(x)^2}\right)} \tag{1}$$

The Gaussian beam radius $\omega(x)$ is the distance from the x-axis at which the intensity has fallen to $1/e^2$ of its peak (axial) value. The value ω_0 will refer to the beam's "waist" radius, the minimal Gaussian beam radius. In free space, there exists a unique beam waist. Assume for the remainder that it occurs at $x = 0$. Thus, the beam expands in

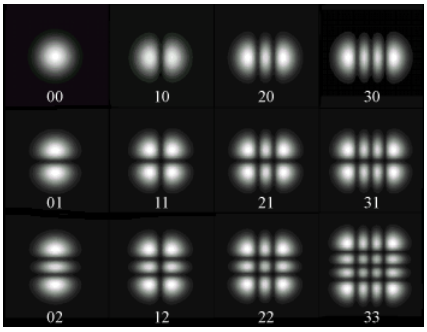

FIGURE 1. Hermite-Gaussian propagation modes

either direction away from $x = 0$. The equation describing $w(x)$ is:

$$\omega(x)^2 = \omega_0^2 \left[1 + \left(\frac{\lambda x}{\pi \omega_0^2}\right)^2\right]. \tag{2}$$

Another property of this beam is the wavefront radius of curvature $R(x)$. At $x = 0$, $R = \infty$, and as $x \to \infty$, $R(x) \to x$. For any x:

$$R(x) = x \left[1 + \left(\frac{\pi \omega_0^2}{\lambda x}\right)^2\right]. \tag{3}$$

These equations can be simplified by introducing the "Rayleigh Range" x_R , the value of x which minimizes $R(x)$. It is also such that $\omega(x_R) = \sqrt{2}\omega_0$. It is given by:

$$x_R = \frac{\pi \omega_0^2}{\lambda} \tag{4}$$

Thus, a pure Gaussian TEM 00 beam is fixed for all x given the location and size of the beam waist ω_0.

For later reference, solving Equation 3 for x_R gives:

$$x_R = \sqrt{(R(x) - x)\, x} \tag{5}$$

2.2. **Fabry-Perot Cavities.** A Fabry-Perot cavity consists of two or more mostly reflective mirrors. See Figure 2 and Figure 3. Light incident upon the input miror is split - most is reflected but some is sent into the cavity. The light in the cavity then falls upon the output mirror - again, most of this remaining beam is reflected back into the cavity. The rest is transmitted.

Call the length of the cavity L. Light taking a round trip through the cavity traverses a total path length p (for perimeter). For the two-mirror cavity shown in Figure 2, $p = 2L$. If the light is such that an integral number of wavelengths fit precisely into this distance p, the light reflecting around inside the cavity will be *in phase* with itself on each successive trip. This is constructive interference - the light will "resonate". In a typical resonating Fabry-Perot cavity, the transmitted light intensity is nearly equal to the input light intensity.

The mode cleaners discussed in this paper are three-mirror "ring" cavities. Such cavities are not fundamentally different than ones with only two mirrors. The total optical path

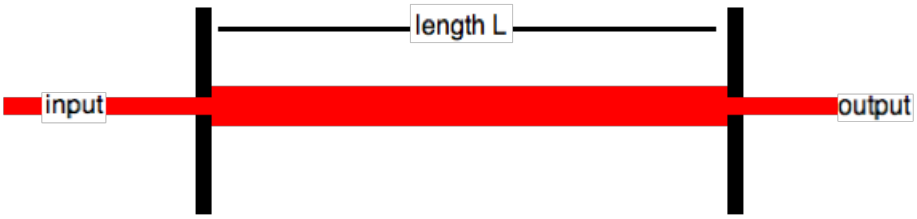

FIGURE 2. Diagram of a 2-mirror Fabry-Perot optical cavity of length L

length p inside the cavity remains the crucial dimension. See Figure 3. We discuss designs with the new vertex mirror located much farther away than the separation of the two 45° mirrors. Thus it is still approximately true that $p = 2L$.

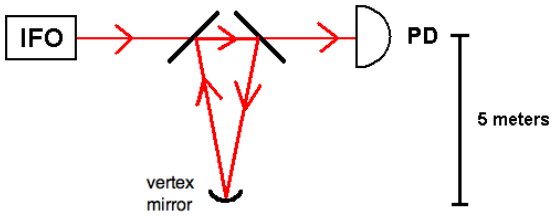

FIGURE 3. Diagram of a 3-mirror Fabry-Perot optical cavity of length 5 meters in use between an interferometer and an output photodiode (PD).

A given cavity's response to light of different frequencies can be easily worked out from the integral-wavelength requirement. Suppose a given wavelength λ_1 resonates in a cavity of perimeter p. Thus

$$p = q\lambda_1,$$

for a positive integer q. Then there exists λ_2 such that

$$p = (q+1)\lambda_2.$$

Substituting for frequencies and subtracting, we have

$$p\,(\nu_2 - \nu_1) = (q+1)\,c - qc = c.$$

The quantity $\nu_2 - \nu_1$ depends only on c and p, and not on q or λ_1. It is the so-called free spectral range (FSR) of the cavity, f_{SR}. It represents the frequency spacing between cavity resonances.

$$f_{SR} = \nu_{i-1} - \nu_i = \frac{c}{p} \tag{6}$$

A mode cleaner that resonates perfectly the LIGO sidebands translates to a Fabry-Perot cavity with free spectral range equal to the radio frequency sideband offset:

$$f_{SR} = f_{SB}. \tag{7}$$

Given the goal of using such a mode cleaner on LIGO's H2 IFO, this becomes $f_{SR} = 29.506876\ MHz$. Solving Equation 6 for the path length p yields $p = 10.16m$ ($L \approx 5m$). Refer to Figure 4.

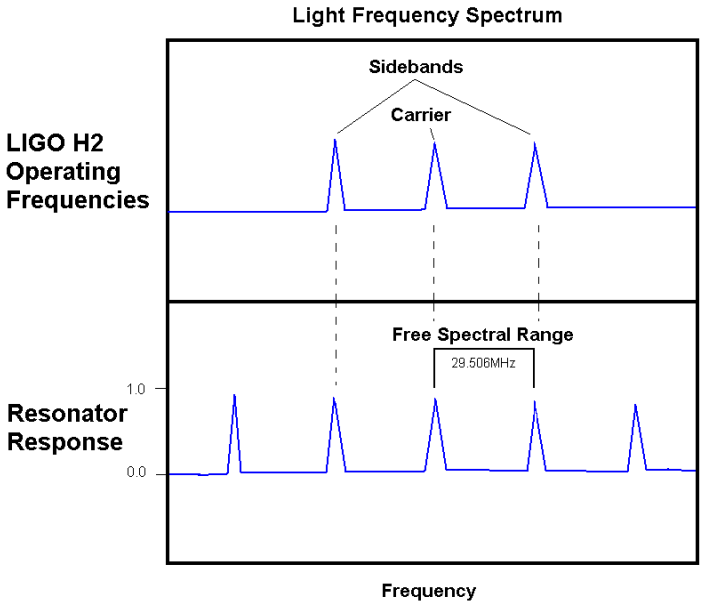

FIGURE 4. Do you need a caption?

Another important cavity parameter is the finesse (F). In a physical cavity, mirror imperfections spread a given resonance around the resonant frequency. The bandwidth Δ_ν of the cavity is usually defined as the full width at half maximum of the cavity transmission as a function of frequency. The finesse is defined as the ratio of the f_{SR} to the bandwidth. Hence it is a type of cavity "resolution". The following formula in terms of cavity losses (gains) can be derived from this ratio (cite Siegman). Define the gain g_i of a cavity mirror i to be the fraction of power reflected at the given incidence. Let g_{rt} be the round-trip gain in the cavity: $g_{rt} = g_1 g_2 ... g_n$.

$$F = \frac{f_{SR}}{\Delta_f} = \frac{\pi\sqrt{g_{rt}}}{1 - g_{rt}} \tag{8}$$

2.3. **Mode Cleaning.** An important characteristic of a mode cleaner is how it treats the various higher-order propagation modes (Section 2.1; Figure 1). Recall that for a LIGO mode cleaner, we seek to resonate only the lowest-order TEM 00 mode. By using a curved mirror in a cavity, one can in a way control the way that higher order modes are resonated. In our case, we use a spherically curved vertex mirror in a three-mirror triangular cavity. See Figure 5. Call the radius of curvature of this mirror's reflective surface R_s.

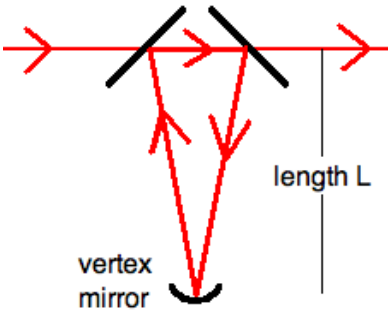

FIGURE 5

Ideally, the goal is to build a cavity such that *no other modes resonate when the 00 mode is resonant.* It can be shown that the resonant frequencies of a given mn Hermite-Gaussian mode in a curved-mirror cavity depend on the radius of curvature of the curved mirror - more specifically, the ratio $p/2R_s \approx L/R_s$, where again p is the total optical path inside the cavity and L is the physical length. From [cite Siegman], it can be shown that for a two-mirror cavity:

$$\nu_{mn} = f_{SR}\left(q + (n+m+1)\,\frac{sin^{-1}\,(p/2R_s)}{\pi}\right) \tag{9}$$

with $q \in \mathbb{Z}$. Subtracting away the 00 mode resonance for a given q yields a frequency difference:

$$\nu_{mn} - \nu_{00} = f_{SR}\,(n+m)\,\frac{sin^{-1}\,(p/2R_s)}{\pi}. \tag{10}$$

In principle, we then need to choose $p/2R_s$ such that $\nu_{mn} - \nu_{00}$ is not an integer multiple of the f_{SR}. Otherwise, the mn mode will overlap with many 00 mode resonances. Since for this project we are constrained by the condition that $f_{SR} = f_{SB}$, p is fixed and R_s is our only remaining degree of freedom.

There is a subtlety with Equation 9 when used with a three-mirror (or any odd number) cavity. The odd number of mirrors introduces an overall π phase shift. This shift moves the resonant frequencies of the odd-m modes (the ones with antisymmetric horizontal phase distribution) by $f_{SR}/2$. Thus, higher-order coincidences with 00 resonance are more common. To account for this, we would like to assure that for such modes, $\nu_{mn} - \nu_{00} \neq integer \times f_{SR}/2$, a more stringent condition than in the preceding paragraph.

We performed a computational study to determine the optimal R_s. We were constrained by the following:

$$p/2 < R_s < p, \tag{11}$$

for stability (no imaginary physical quantities), and

$$R_s \in \mathbb{Z} \tag{12}$$

with R_s in meters, in order to obtain a mirror sufficiently quickly (suppliers typically only have integer-meter radii of curvature in stock for such large R_s). Thus, we considered $R_s = 6\ m, 7\ m, 8\ m, 9\ m$, or $10\ m$. We allowed for $R_s \pm 0.5\%$. Our criterion for overlap was that a mode mn be within three bandwidths $\Delta_f = f_{SR}/F$ of a 00 mode. Based on mirror losses, we estimated a finesse F of approximately 100. We searched $m + n < 20$. Note that larger $m + n$ resonate with rapidly decreasing intensity. $R_s = 8.0$ yielded the best performance, with an overlap for $m + n = 16$ and possibly at $n + m = 11$ within the range of uncertainty on R_s for our mirror.

2.4. **Other Optics.** In this section, I describe for reference several other key optical elements used during this study.

A lens focuses (or defocuses) light. For a Gaussian beam, a lens alters the wavefront radius of curvature without altering the beam size at the lens. The focal length f is the crucial quantity. For a mode cleaner, lenses are used primarily for mode-matching; a curved-mirror cavity implies a specific beam size and waist location. For optimal performance, a lens (or several) must be used to prepare the input beam to match these properties. To select an appropriate lens, the following formula (the lensmaker's formula) is useful:

$$\frac{1}{f} = \frac{1}{R_i} + \frac{1}{R_o} \tag{13}$$

where R_i is the wavefront curvature radius of the incident beam, and R_o is the desired new wavefront curvature radius. Used in conjunction with the Gaussian beam dynamics in Section 2.1, this formula determines the necessary mode-matching lens focal length and location(s).

A variable half-wave plate (abbreviated $\lambda/2$) rotates the polarization of linearly polarized light by a chosen angle. Depending on the types of coatings used on cavity mirrors, a given mode cleaner will have have greatest transmission at a specific linear polarization. (The same is true for other optical elements as well).

A polarizing beamsplitter cube (abbreviated $PBSC$) splits light into two orthogonally polarized beams. Transmitted light is horizontally polarized (p-polarization), and reflected light is vertically polarized (s-polarization).

An electro-optic modulator (abbreviated EOM) is a crystal which can be driven by an RF signal to rapidly modulate the amplitude or phase of an incident light beam. This is a device for putting *sidebands* on the carrier beam. For our OMC, we use *phase* modulation to put sidebands on the light input to the cavity. This works as follows: Suppose the carrier signal has frequency ν_0 and we wish to incite sidebands offset by f_{SB}. The carrier's field without modulation is:

$$\mathbf{E} = sin\left(2\pi\nu_0 t\right).$$

Adding phase modulation at frequency f_{SB} means the signal becomes:

$$\mathbf{E} = sin\left(2\pi\nu_0 t + \Gamma sin\left(2\pi f_{SB} t\right)\right) \tag{14}$$

where Γ represents the strength of modulation. By expanding the sin, one gets

$$\mathbf{E} = sin\left(2\pi\nu_0 t\right) cos\left(\Gamma sin\left(2\pi f_{SB} t\right)\right) + cos\left(2\pi\nu_0 t\right) sin\left(\Gamma sin\left(2\pi f_{SB} t\right)\right).$$

Assuming that Γ is small and Taylor expanding, we get:

$$\mathbf{E} = sin\left(2\pi\nu_0 t\right) + \Gamma cos\left(2\pi\nu_0 t\right) sin\left(2\pi f_{SB} t\right).$$

And rewriting the second term in terms of sin only, we get:

$$\mathbf{E} = sin\left(2\pi\nu_0 t\right) + \frac{\Gamma}{2}\left[sin\left(2\pi\left(\nu_0 + f_{SB}\right)t\right) - sin\left(2\pi\left(\nu_0 - f_{SB}\right)t\right)\right]. \tag{15}$$

This equation clearly represents sidebands and the frequency content shown in the upper panel of Figure 4.

A photodiode (abbreviated PD) records the DC light level incident on its active surface. A radio-frequency photodiode (abbreviated RFPD) records the DC light level and also outputs the RF oscillating signal.

For reference, Table 1 at the beginning of this section includes the abbreviations introduced up to this point.

Table 1. Summary of Abbreviations

Abbreviation	Quantity or Device	Section
IFO	Interferometer	1
OMC	Output Mode Cleaner	1
ν_0	Carrier Frequency	1, 2.4
f_{SB}	Sideband Offset Frequency	1, 2.4
$\omega(x)$	Gaussian Beam Size (radius)	2.1
$R(x)$	Gaussian Beam Wavefront Radius of Curvature	2.1
f_{SR}	Free Spectral Range of Cavity	2.2
p	Total Optical Path Length in Cavity	2.2
L	Simple Cavity Length	2.2
F	Finesse of Cavity	2.2
Δ_f	Resonance Bandwidth of Cavity	2.2
R_s	Spherical Vertex Mirror Radius of Curvature	2.3
f	Lens Focal Length	2.4
$\lambda/2$	Variable Half-Wave Plate	2.4
PBSC	Polarizing Beamsplitter Cube	2.4
EOM	Electro-Optic Modulator	2.4
PD	Photodiode	2.4
RFPD	Radio Frequency Photodiode	2.4

3. Description of Folded OMC

In this section, I describe the general set-up of our folded OMC cavity.

3.1. **Folded Construction.** In order to readily seat an OMC on a LIGO optical table (e.g. ISCT10 for H2 IFO), it should be less than one meter in length. Our strategy is to add two mirrors to the basic triangular design introduced in Section 2.2, creating a Herriot "delay line" within the Fabry-Perot cavity. This allows the light to traverse a significantly longer path as it bounces back and forth between the "folding" mirrors (F1 and F2 in all following figures). Compare the two images in Figure 6.

We sought to construct this cavity using mirrors in available sizes (0.5 inch, 1 inch, 2 inch). The first step was to determine exactly how this might work. A successful arrangement is as follows (consult the bottom panel of Figure 6). Mirrors A and B are 1 inch in diameter. Mirror C is 1/2 inch in diameter. And mirrors F1 and F2 are each 2 inches in diameter. Light enters the cavity by passing through mirror B, whose surface is aligned at 45° to the beam path. Mirrors A and B are 98.5% reflective at 45°*incidence*, so most of the light is reflected away from the cavity. The light which entered the cavity reflects off of mirror A (some is transmitted) and passes over mirror F2. The beam bounces back and forth between F1 and F2, striking F1 three times and F2 twice. It than passes underneath mirror F2 near the horizontal center, striking mirror C, the spherical vertex mirror of the cavity. The light then reflects back underneath F2 and back and forth between F1 and F2 again. The beam returns to mirror B by passing over F2 once again. In an aligned cavity, the beam perfectly overlaps itself (in phase) on repeated passes, causing resonance.

Figure 7 contains two sketches made when trying to determine a useable arrangement. The top panel is an axial view of the cavity's mirror. The center of the image is near the centers of the folding mirrors F1 and F2. If we assume that mirrors A, B, C, and F2 are clustered closer to the viewer (with F1 farther away into the page), the beam enters the cavity at the upper left spot and reflects off of the upper right mirror (mirror A) towards the far folding mirror F1, marked with a red spot in the figure. This image is the result of a parameter search to determine what geometries were possible. For example, varying the distance between mirrors A and B, the height of those mirrors above mirror C, or the axial distance between the various elements, results in different spot patterns.

Our criterion for this study was that 99.99% of a beam's power must fall on a mirror's reflective surface. To determine the beam sizes, we must know the cavity's characteristic waist size. We assume that it occurs at the cavity entrance. The other condition is that the beam's wavefront radius of curvature is $8.0m$ at the curved mirror (C) approximately five meters away. This will optimize the cavity's effectiveness as a resonator. From Equations 4 and 5,

$$x_R = \frac{\pi\omega_0^2}{\lambda} = \sqrt{(8.0m - 5.1m)\,5.1m}$$

Solving this equation gives $\omega_0 \approx 1.1\ mm$. The beam size at every point in the cavity can now be determined. In particular, this implies a beam size of $\approx 1.9\ mm$ at the vertex mirror C.

For each proposed geometry, the beam sizes were computed at the location of each mirror. Integrating the beam intensity profile (Eq. 1) gives the fractional power within an aperture a for a beam with size ω:

$$\frac{P(a)}{P(\infty)} = \left[1 - e^{\left(\frac{-2a^2}{\omega^2}\right)}\right]$$

Our requirements, and the beam contours in red and blue drawn in Figure 7, correspond to

$$\frac{P(a)}{P(\infty)} > 0.9999$$

3.2. **Mode Matching and Table Arrangement.** Mode matching refers to placing the appropriately sized beam (1.1mm) at the entrance to the OMC cavity. It was not a major priority for this initial study. We implemented a one-lens system with a focal length

different from the optimal value by about 10% (because it was available). To determine the approximate lens placement, we propagated beam waists forward from the laser and backward from the cavity entrance. At the location where the two beams are the same size, we put a $f = 1m$ lens (the optimal computed value is 914 mm).

Figure 8 is a diagram of our latest OMC test setup, including input and output elements. An NPRO laser was used at 1.06 microns. We used three video cameras to monitor the cavity: one viewed the output light directly. Another faced the back of the folding mirror F1 in order to readily track the beam spots during alignment and observation. The third was placed above the cavity to get a view of the survace of the spherical vertex mirror C. PDA55 photodiodes were used to observe both the transmitted laser light and the light reflected off the cavity (mirror B). A radio frequency photodiode (RFPD) was used to analyze the cavity's treatment of the RF sidebands.

Variable half-wave plates are used to optimize the beam's polarization for the downstream optical elements. The EOM and cavity require precise polarization.

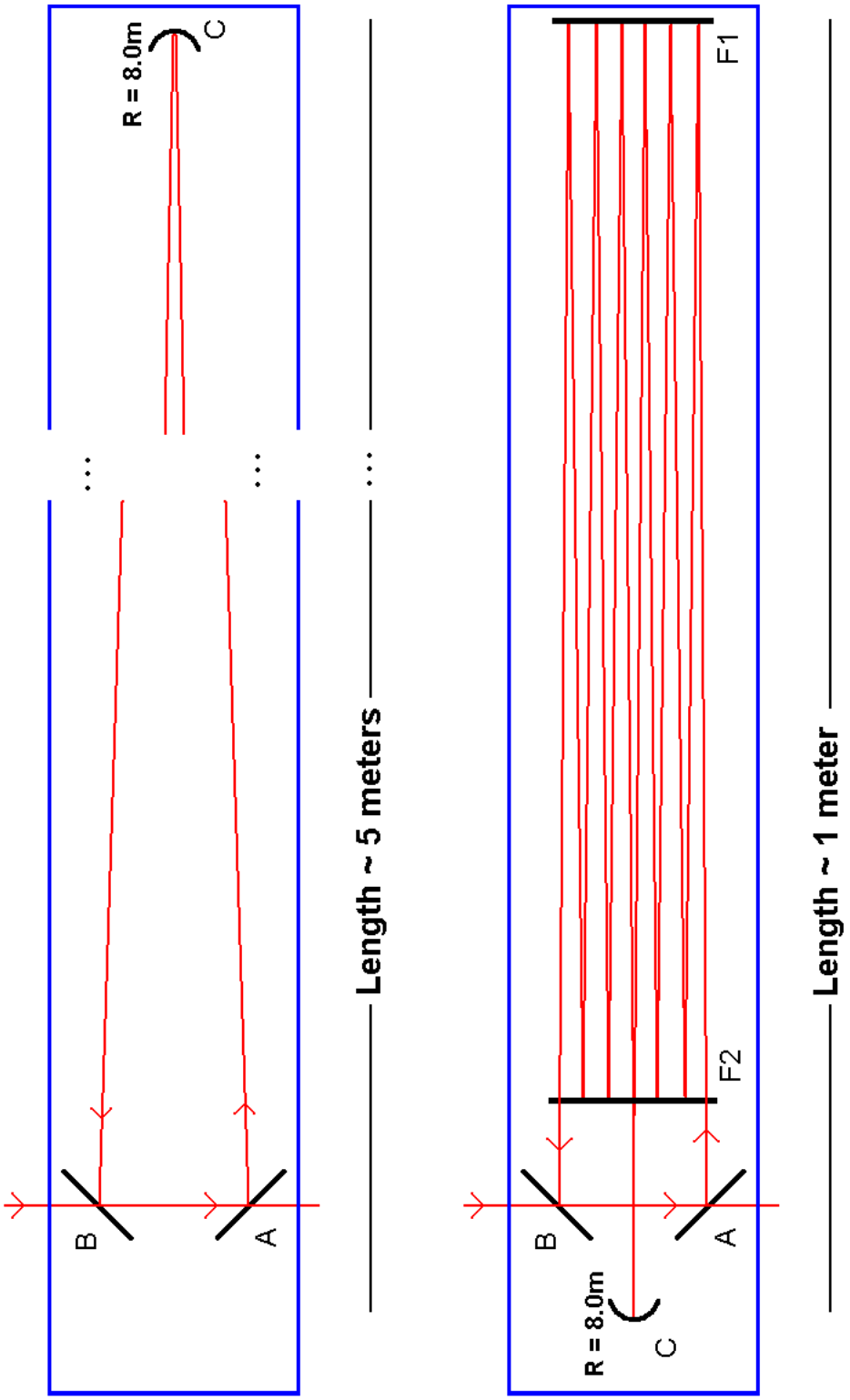

FIGURE 6. Comparison between folded and unfolded OMC cavity designs, viewed from above. Top: Simple 3-mirror cavity - requires a 5-meter cavity to resonate the sidebands. Bottom: A "3-fold" Folded cavity need only to be ≈ 1 meter long.

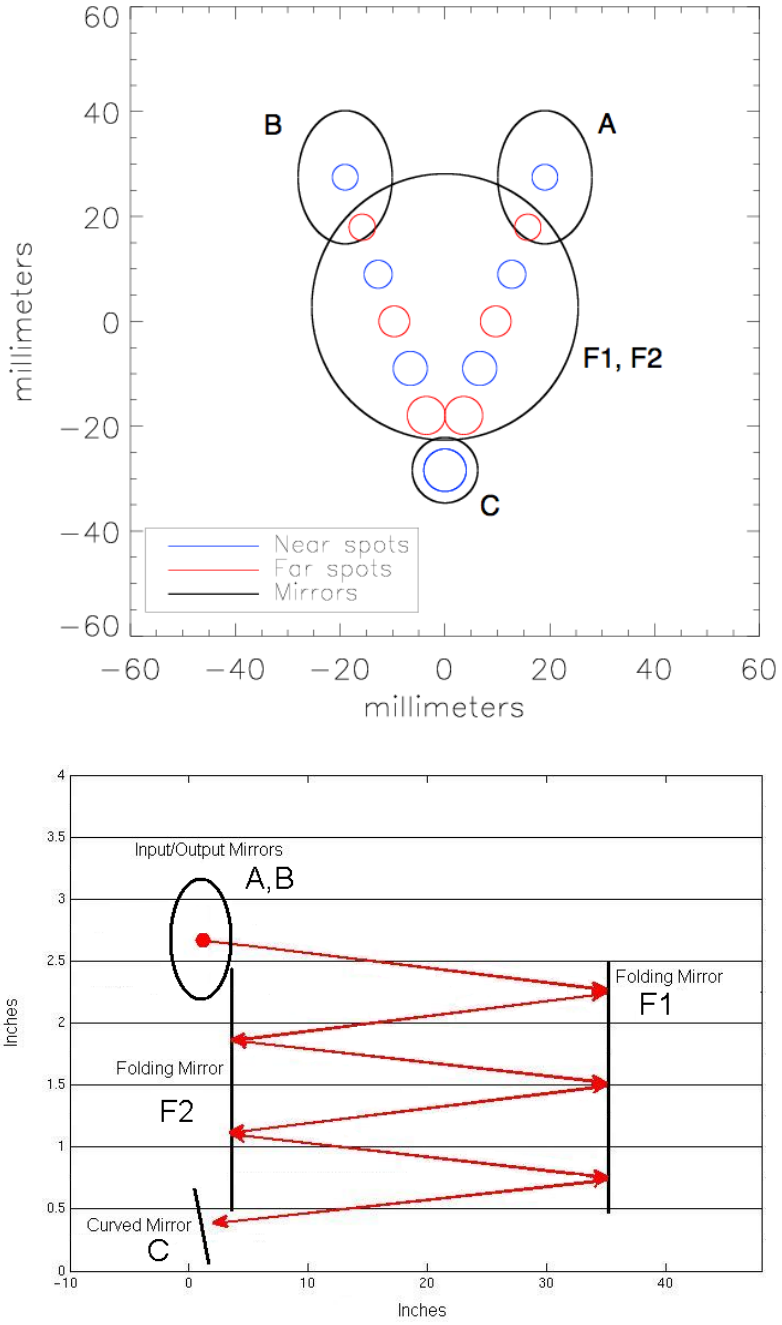

FIGURE 7. Diagram of the axial and side views of our proposed OMC cavity. These diagrams were used to determine feasible and useful mirror setups.

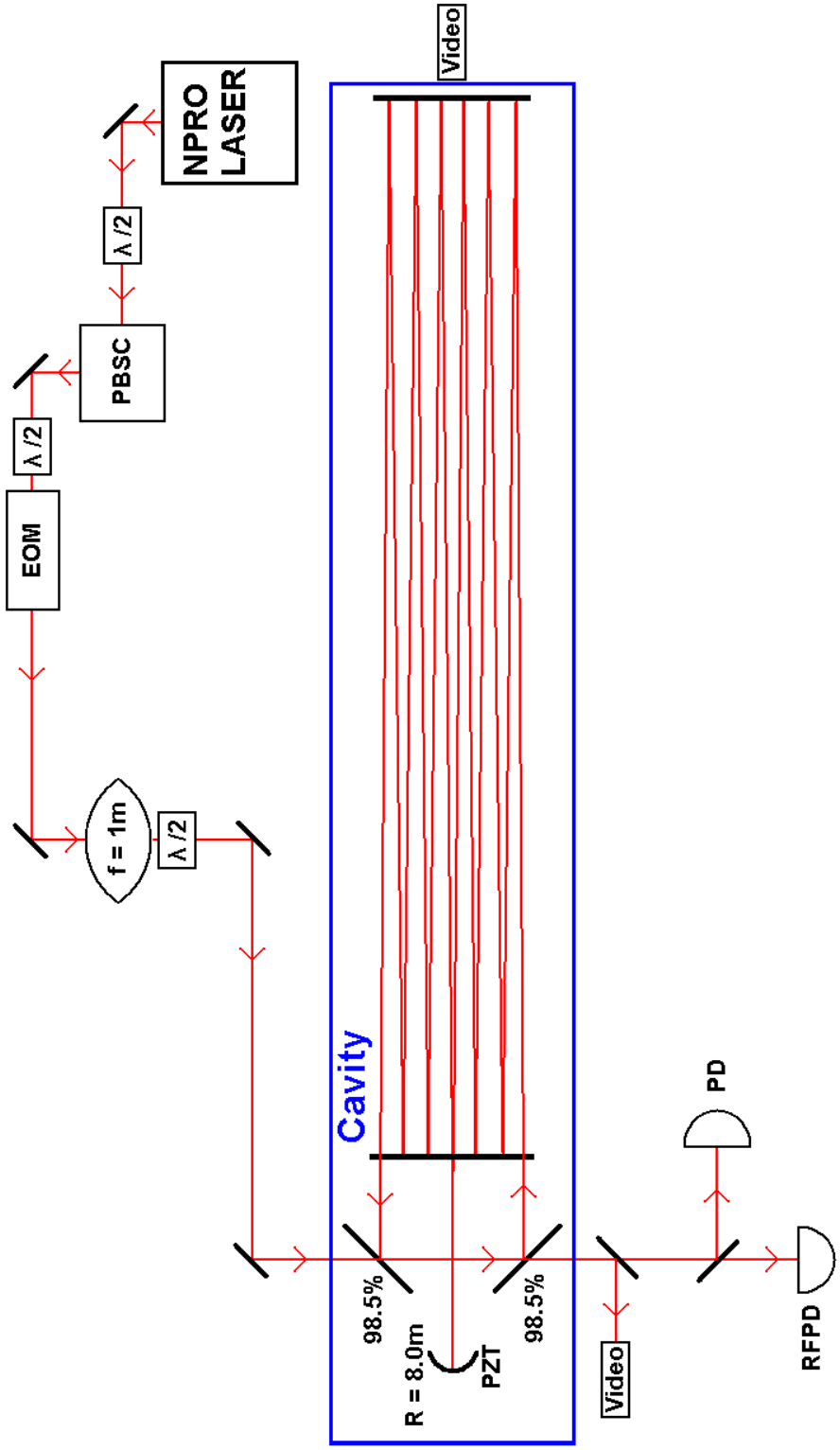

FIGURE 8. Diagram of the OMC cavity test setup, including input and output optical elements.

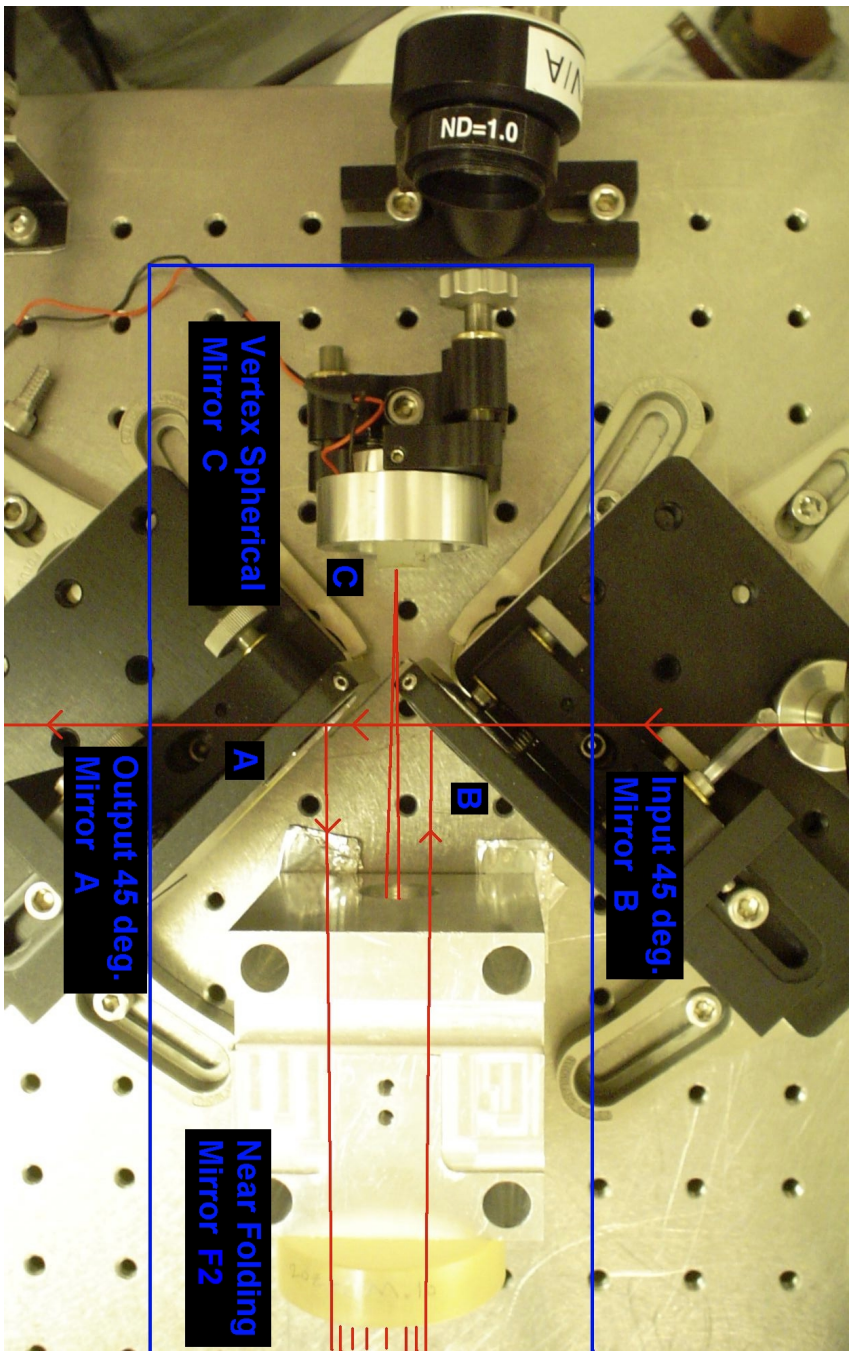

FIGURE 9. Photograph of the four nearby mirrors A, B, F2, and C at the cavity input/output. Red lines are the approximate beam path.

4. Lock Methods

A mode cleaner cavity will not maintain a resonance on its own. A mode cleaner is extremely sensitive to changes in length and microscopic misalignments of its mirrors. Seismic noise, acoustic noise, and temperature variations can alter the cavity length and/or alignment so that it is no longer on resonance. For example, our test cavity was built on a stainless steel optical table. The coefficient of thermal expansion α of stainless steel is 1.7×10^{-5} $(^{\circ}C)^{-1}$. For a slow instantaneous rate of temperature change such as $1^{\circ}C$ per hour, this corresponds to roughly $\Delta p = 1.5\ nm\ s^{-1}$ of optical length change for our folded cavity. Over a few minutes this is enough to alter the path length by a significant portion of a wavelength. Seismic shocks and acoustics (e.g. talking) have even more drastic effects.

To keep a cavity locked, a locking system or servo must be used. Without it, a cavity will only "flash" - resonate briefly in various modes as the cavity changes or "breathes". For our cavity, we implemented a "dither" lock, which locks to a carrier resonance by maximizing the DC throughput of the cavity. This is discussed in 4.1. We also investigated a carrier-independent RF locking scheme (Section 4.2) which locks to the $2f_{SB}$ output signal. In other words, it attempts to maximize the signal of the sidebands beating with each other.

4.1. **Dither Lock.** A dither lock servo makes tiny adjustments to the cavity's length based on the amplitude of transmitted light. The cavity is connected to the servo loop in two ways: the output light falls on a photodiode, and a piezoelectric transducer (PZT) stack is affixed to the spherical vertex mirror (C). A PZT stack is composed of many sheets of piezoelectric material. Such materials convert electrical signals into microscopic mechanical movements. (They can also do the opposite). Thus, the length of our cavity can be carefully controlled and a resonance sustained.

The details of the dither lock are as follows. Refer to Figure 10. A signal generator drives (dithers) the PZT with a tiny sinusoidal voltage. In our final configuration, we used a frequency of 9 kHz at a few μV. The cavity's DC output signal from a photodiode (PDA55) is sent to a lock-in amplifier. The lock-in synchronizes to the dither frequency via a "sync" from the signal generator. It then performs a multiplication of the (DC) light signal with its synchronized oscillator, and averages over time. It computes an "error signal" which the servo is designed to null. The output of the lock-in is a DC offset which is added to the PZT dither signal (with a possible inversion). To see how this works, assume the cavity is on resonance. As the PZT dithers in either direction, the cavity's output light falls because its length is moving away from a 00-mode resonance. The lock-in amplifier can identify this tiny 9 kHz signal. If the resonating cavity is not changing, it will generate equal-magnitude, opposite-direction error signals as the dither moves back and forth, negating any overall PZT offsets and maintaining the resonance. However, if the cavity's length is changing by some external effect, the lock-in will generate more error signal for one dither direction than the other. The lock-in output signal then pushes the PZT in the direction which negates this change by applying an appropriate voltage.

4.2. **RF Lock.** A locking scheme was devised which is independent of the carrier signal. This property could be desirable since the LIGO carrier signal is intentionally nulled by the PDH locking servo, and is potentially erratic and noisy due to IFO operation. This scheme takes advantage of the sidebands beating with each other, yielding RF power at a frequency of $2f_{SB}$. This RF power from the RF photodiode is filtered (to reduce noise from

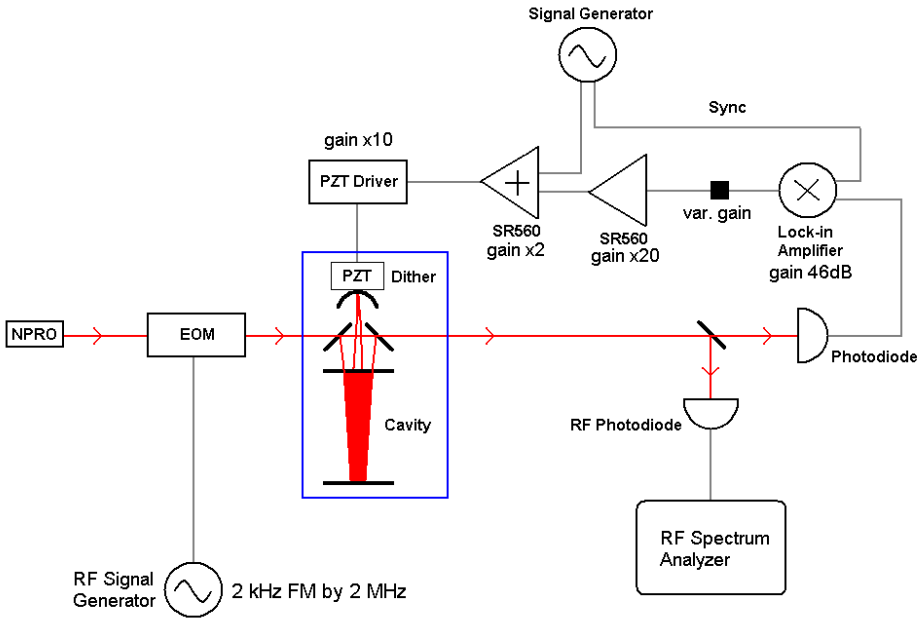

FIGURE 10. Our dither lock servo. Red lines are laser light, grey lines are electrical signals (BNC connections). A triangle represents a signal amplifier.

signals not at $2f_{SB}$), amplified, and demodulated by an RF mixer. This process results in a DC signal proportional to the amplitude of the $2f_{SB}$ power, which is then sent to a lock-in amplifier. See Figure 11

To create a dither signal, the EOM is driven with frequency modulation (FM). Thus the frequency of the sidebands themselves oscillates rapidly around the cavity's FSR. The rest of the lock system operates identically to the dither lock in the preceding section. If the cavity's FSR matches exactly the EOM center driving frequency, the frequency modulation causes the amplitude of the sideband power to fall equally when the driving frequency moves away from center in either direction. As the cavity changes, the lock-in detects the error, and corrects it by driving the PZT with a small voltage to offset the change.

This method has several potential advantages. As mentioned above, it is carrier independent: no matter what happens to the carrier signal within the IFO, the locking method will perform identically. It depends only on the sidebands, which are not affected by the IFO arms. Another potential advantage is that it involves less physical movement of the cavity itself. The rapid dither (above about 6 kHz) of the PZT creates some minor but audible acoustic noise. The RF lock described here reduces the movement to just slower PZT offsets.

At the time of this writing, these potential advantages have not been extensively tested. It is hoped that as the work continues on the test OMC cavity, the relative merits will become known.

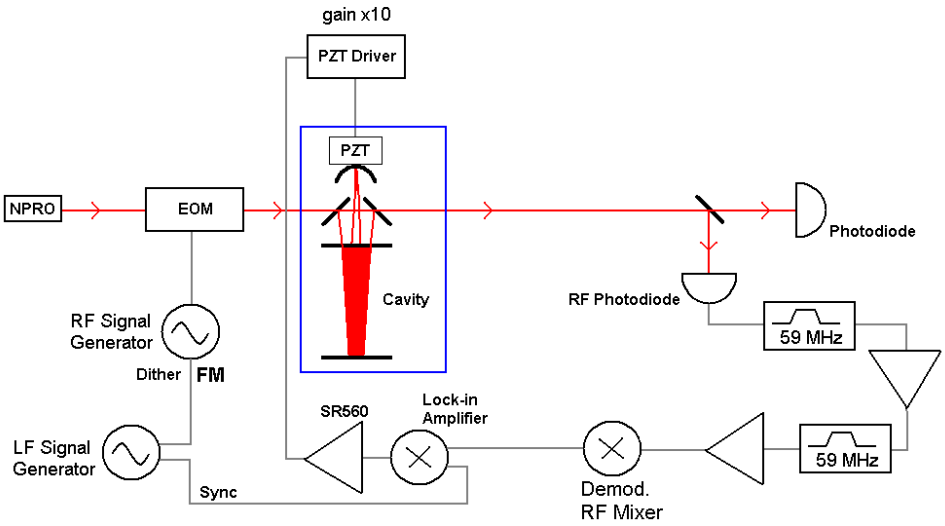

FIGURE 11. Our RF locking servo. Red lines are laser light, grey lines are electrical signals (BNC connections). A triangle represents a signal amplifier.

5. Observations

This section contains initial observations of our OMC cavity. We used with the standard dither lock of Section 4.1. I describe observations of locking effectiveness, noise, and stability. An RF measurement of the cavity's FSR is presented. We make initial diagnostic measurements of cavity noise effects on frequency sidebands near the FSR.

5.1. **Noise Observations.** Our initial locking cavity suffered from pervasive noise. To test the noise of the cavity, we used a guassian laser beam (1024 nm) incident on the cavity and observed the direct signal on the photodiode as well as the power spectrum. Full attenuation was observed at $\approx 60\ Hz$ and $\approx 440 Hz$.

This first cavity model (let's call it Cavity A) was built without perfect attention to optic element stability. We built a new model (Cavity B) using larger and stronger optic mountings. See Figure 12 for a look at our mounts. We were able to measure the resonant frequency $\approx 720\ Hz$ of the improved mount for mirror F2 by attaching various masses. This increase in resonant frequency is observed in the noise-induced attenuation of the output spectrum. The 440 Hz signal was replaced by the 720 Hz signal. Since the physical amplitude tends as $1/f^2$, this represents a reduction in signal disruption due to this noise.

In fact, the new mounts reduced the observed locked attenuation substantially, to about 5% of the total signal (see Figure 13). We also discovered an important dependence on signal noise and throughput on the beam's clearance through the EOM. Our sideband frequency and curved mirror requirements imply a relatively large beam input size ($\omega \approx 1.1mm$), so care must be taken to avoid the beam clipping the small aperture (2mm) of the EOM prior to cavity incidence.

Much effort was spent optimizing the locking servo. Precise gain control in the servo is essential. Too much gain in the servo causes large attenuation in the output signal at the *dither frequency*. Too little gain in the servo causes large low-frequency attentuation and

frequent breaks of lock. This effective gain window has width of less than approximately 10%. A varying signal strength (on the photodiode) necessarily varies the total gain in the servo. Hence, the effective downstream (from the photodiode) gain depends on the absolute signal throughput.

The locking servo and the noise in the output signal were both highly dependent on the environment. Footsteps, voices, loud noises, brushing against the optical table all produced catastrophic noise and often broke lock. We expect that these effects would be vastly improved by 1) seismically isolating the table, 2) putting the cavity within a foam or plastic encasement, and 3) permanently gluing the mirrors into their mounts.

5.2. **RF Measurements.** The free spectral range of the cavity can be measured by observing the RF power transmitted by the cavity while scanning the sideband frequency. The EOM puts sideband on our laser signal via phase modulation. However, if $f_{SB} \neq f_{SR}$ of the cavity, some of this phase modulation is converted into amplitude modulation at the same frequency f_{SB}. This amplitude modulated signal is detected by the RF photodiode. Thus, scanning the RF sideband frequency produces an RF output spectrum with an obvious dip. The minimum of the dip occurs at $f_{SB} = f_{SR}$ because the conversion to amplitude modulation is minimized there.

Figure 14 is an example of such a measurement. In this case, f_{SB} was frequency modulated by 2 MHz at 2 kHz using an RF signal generator. The RF spectrum was observed using an RF spectrum analyzer which scans the spectrum at much slower than 2 kHz and averages. Thus, the spectrum displayed represents the "smeared" signal as f_{SB} oscillates. The best guess f_{SR} for this cavity (version B, with the new mounts) from this measurement was 29.6 MHz.

Initial measurements of the cavity's RF noise behavior were taken. Consider the $2f_{SB}$ power output signal (the same used in the RF dither lock in Section 4.2). Noise processes induce sidebands on this signal. For example, the same signals as seen in the PD output signal of 5.1 are seen as sidebands on this $2f_{SB}$ signal at 60 and 720 Hz, respectively.

To determine the noise behavior of the cavity with RF sidebands near f_{SR}, multiple measurements of these noise-induced sideband peaks were taken. Incrementing the sideband frequency by 1 kHz very near the estimated f_{SR} mentioned above, the center peak powers of the noise-induced sidebands were compared to the center peak power of the $2f_{SB}$ signal. This data is presented in Figure 15 for the frequencies ≈ 60 Hz (later determined more likely to be 59 Hz) and ≈ 720 Hz. Note: the peak power of the $2f_{SB}$ signal remained effectively constant within this range of sideband frequencies (about 10 kHz).

6. Summary

blah blah

7. Acknowledgements

I owe my deepest gratitude to Dr. Richard Gustafson for advising this project and providing an enormous amount of attention to me and this project all summer. Also thanks to Dr. Rick Savage, Dr. Keita Kawabe, and Dr. Paul Schwinberg for providing valuable help on this project throughout the summer. Additional thanks to: Terry Gunter and of course all the staff at the LIGO Hanford Observatory; The California Institute of Technology; and the National Science Foundation.

References

[1] Siegman, A., *Lasers*, Mill Valley, CA: University Science Books, 1996
[2] Kawabe, Keita, *Design and Performance of the Output Mode Cleaner*, LIGO G040326-00-D
[3] Saulson, Peter, *Fundamentals of Interferometric Gravitational Wave Detectors*, World Scientific, 1994

Appendix A. Alignment

For reference, I include some observations regarding alignment of the OMC cavity.

A.1. **Vertical Motion of the Beam Spot on the Spherical Mirror (C).** It is desirable to center the beam spot on the vertex mirror. This improves the stabilizing and mode-cleaning properties of the spherical mirror, as well as the finesse of the cavity (because less power falls off the mirror).

To achieve vertical displacements of the (aligned) beam on the vertex mirror C, the following method is effective. This technique should be used when the cavity is aligned and locking robustly and one wishes to move the beam spot *downwards*. The obvious changes to the method will allow one to move it upwards as well. It uses observations made with the output photodiode and video camera placed behind folding mirror F1. "Maximizing" the output photodiode means adjusting the mirror alignment until the 00-mode flashes achieve the largest amplitude.

Step 1. Tilt beam downwards using the far folding mirror F1. The locking will fail and the 00-mode resonances will dramatically drop in amplitude. Tilt downwards until the bottom two spots behind F1 (as seen on video) are no more than 1/2 way off the bottom of the mirror.

Step 2. Maximize the output photodiode using the spherical vertex mirror C. You will have to tilt the beam upwards to achieve alignment (beam coincidence throughout the cavity). You should be able to recover most of the output resonance amplitude on the photodiode, and the cavity will regain locking behavior.

Step 3. During a lock, maximize the output PD using the farthest effect pre-cavity steering mirror. You should clearly see the output power rise and fall with tiny adjustments to the pre-cavity alignment. If you move too far in any direction, you will have to slowly search until you regain proper alignment so that locking will occur.

Step 4. Maximize PD output again using the spherical vertex mirror C. If the initial location of the spot on mirror C was poor enough, you should now see noticably larger power during 00-mode resonances and locks.

Step 5. Adjust gain in the locking servo to minimize noise due to change in overall signal strength.

Step 6. Repeat as necessary.

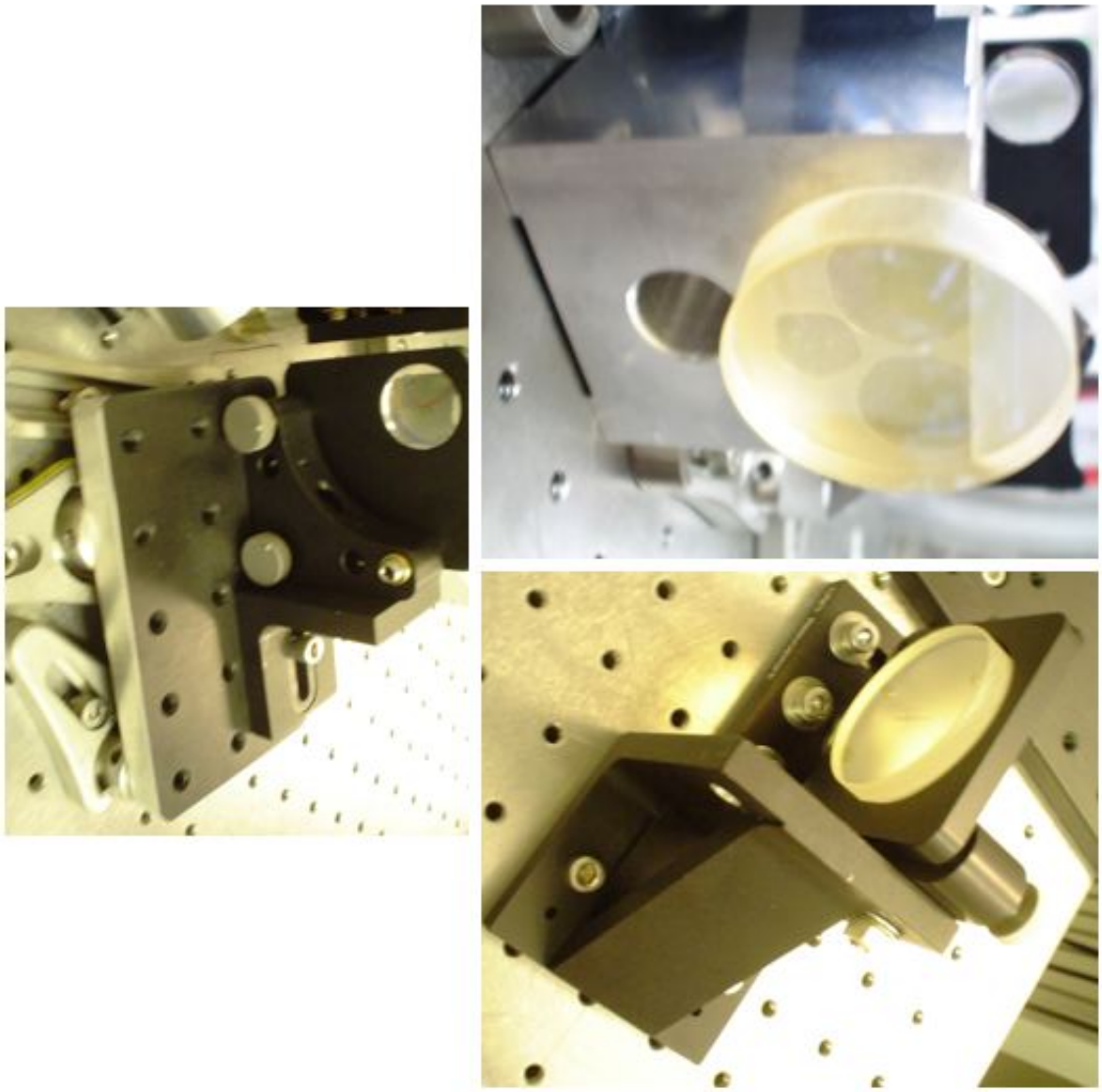

FIGURE 12. Latest version of the OMC optic mounts.

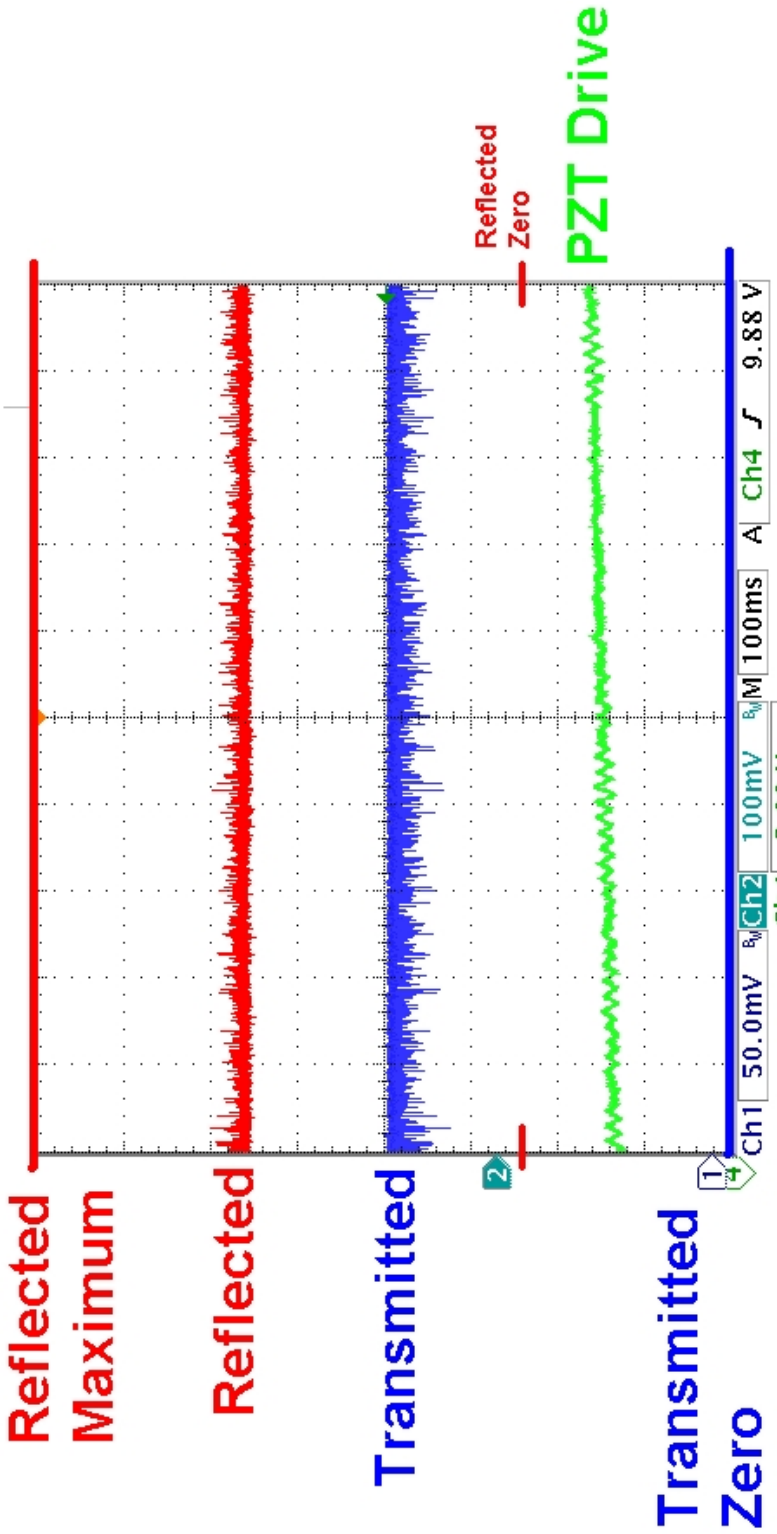

FIGURE 13. example caption

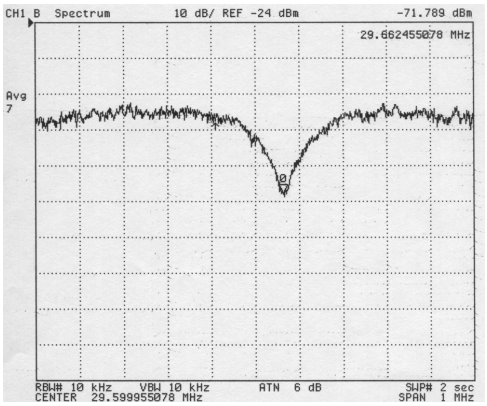

FIGURE 14. Free spectral range (f_{SR}) measurement.

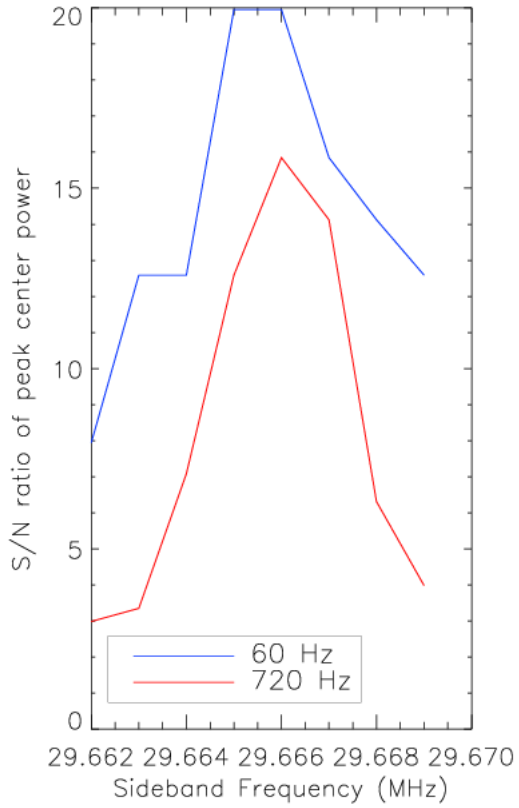

FIGURE 15. Measurement of the noise-induced sidebands at $\approx 60\ Hz$ and $\approx 720\ Hz$ visible in the $2f_{SB}$ OMC output power. The SN ratio is computed by comparing the power at the center of the signal peak to the power in the center of the sideband peak.